scientific reports

Check for updates

OPEN

Identification and verification of XDH genes in ROS induced oxidative stress response of osteoarthritis based on bioinformatics analysis

Chengze Qiu[1], Zhiyong Zhang[1], Haocheng Wang[1], Na Liu[2], Ruixin Li[1], Zhiheng Wei[1], Benjie Wang[1] & Nan Zhang[1]✉

The purpose of this study was to search for genes related to ros induced oxidative stress in osteoarthritis(OA) cartilage through bioinformatics analysis, and to verify the expression of related genes in articular cartilage of OA patients. OA expression data and ROS-related genes were downloaded from GEO (GSE51588, GSE117999) and Molecular Signatures Databases. The limma package in R language was used to screen differently expressed genes (DEGs) from the GEO databases. WGCNA analysis and Venn diagrams were employed to screen genes that were differentially expressed between OA and control samples and had strong correlations with ROS as candidate genes. DEGs were screened by GO and KEGG enrichment analysis, as well as protein-protein interaction (PPI) analysis. Besides, the software Cytoscape and database STRING were utilized to screen hub genes networks. The hub genes were confirmed by analysis of the receiver operating characteristic (ROC) curve on the GSE51588 and GSE117999 databases. An artificial neural network model was constructed for the hub genes, and immune analysis was conducted using the ssGSEA algorithm. The expression of genes in OA and normal chondrocytes was verified through HE staining, immunohistochemistry, ROS detection, qRT-PCR and Western blotting test. This study identified five genes, including ALB, CDH1, HSPA8, HIST1H2BE and XDH, as hub genes. ROC curves, gene expression analysis, and artificial neural network diagrams indicated that ALB, HIST1H2BE and XDH had good diagnostic characteristics. GSEA showed that the XDH gene was significantly enriched in ROS pathways. Meanwhile, the expression of XDH were also confirmed to be significant differences between injured cartilage and normal cartilage in OA patients in vivo. Our study may provide new hub genes related to ROS-mediated oxidative stress in OA and validate the correlation between XDH gene and its transcripts with ROS pathways in OA. This offers potential clinical applications for understanding the pathology, diagnosis, and treatment of OA.

Keywords Osteoarthritis, Reactive oxygen species(ROS), Oxidative stress, Xanthine dehydrogenase(XDH), Bioinformatics analysis

Osteoarthritis (OA) is a chronic degenerative disease that causes significant public health problems worldwide, and it is one of the leading causes of disability and widely affects the quality of life of patients in most countries[1,2]. The primary pathological features of OA include degeneration and damage of articular cartilage, pathological changes in adjacent subchondral bone, synovium, muscles, and surrounding adipose tissue, leading to joint pain, swelling, stiffness, and limited function[3]. These symptoms severely impact patients' physical and mental health and daily life, exacerbating the social burden. Currently, there is a lack of effective treatment options for OA, with most therapies aimed at reducing and controlling symptoms and alleviating pain rather than truly slowing down the pathological progression of the disease. As a result, most patients ultimately require total knee replacement surgery to restore joint function, which imposes significant physical and emotional pain as well

[1]Department of Orthopedics, Affiliated Xinhua Hospital of Dalian University, Dalian 116000, Liaoning, China. [2]Department of Hematology and Rheumatology, Affiliated Xinhua Hospital of Dalian University, Dalian 116000, Liaoning, China. ✉email: zhn1979-08@163.com

as heavy financial burdens on patients. Therefore, it is necessary to further deepen our understanding of the pathogenesis of OA and develop targeted treatment methods.

Oxidative stress is a redox reaction that occurs when the level of reactive oxygen species (ROS) exceeds the cell's antioxidant scavenging capacity. ROS are a class of highly reactive oxygen-containing molecules and free radicals, including superoxide anion (O_{2-}), hydrogen peroxide (H_2O_2), hydroxyl radical (-OH), and nitric oxide (NO). They play a dual role in biological systems, participating in normal physiological processes and also contributing to damage under pathological conditions. ROS in physiological concentration is widely involved in a variety of cell physiological functions, and is an important cellular messenger regulating normal signal transduction, gene regulation and cell cycle, and is crucial for maintaining normal cell function[4]. However, due to their high reactivity, the high and sustained concentrations of ROS can cause damage to many cellular and extracellular constituents, including DNA, proteins and lipids[5–7], which will directly cause inflammatory responses in tissues and organ. It has been reported that ROS-mediated oxidative stress generated by polymorphonuclear neutrophils (PMNs) at the site of inflammation causes the opening of interendothelial connections and promotes the migration of inflammatory cells across the endothelial barrier[8]. The migrated inflammatory cells not only help in the clearance of pathogens and foreign particles but also lead to tissue injury.

Oxidative stress is a key driver in OA pathophysiology: elevated intracellular ROS disrupts cartilage homeostasis, causing ECM loss, cell aging, mitochondrial dysfunction, chondrocyte apoptosis, and subchondral bone loss, thereby accelerating OA progression[9–12]. ROS further promotes OA via signaling pathways (e.g., PI3K/Akt, JNK, ERK) and inflammatory responses: it induces chondrocyte apoptosis/dedifferentiation and triggers infiltrating immune cells to release pro-inflammatory factors (e.g., IL-1β, TNF-α, IL-6), which in turn amplify ROS production and matrix-degrading protease expression, exacerbating cartilage damage[13–16]. Thus, excessive intracellular ROS is critical to OA pathogenesis.

Although a large number of studies have demonstrated the influence of ROS in chondrocytes on the occurrence and development of OA, but the current research on the key genes and related proteins that affect the production of ROS is limited, and the mechanism leading to the excessive production of ROS in chondrocytes is still unclear. In this study, we used bioinformatics analysis to identify differentially expressed pivotal genes and investigated their biological functions and regulatory mechanisms. Finally, the role of transcriptase in ros mediated oxidative stress was verified by detecting the expression of related genes in injured cartilage of OA patients. These findings may provide new insights into the molecular mechanisms of osteoarthritis and further offer diagnostic biomarkers and therapeutic targets for osteoarthritis.

Materials and methods

Data collection

The data used include GSE51588 and GSE117999. Both of them are from the GEO database, with the website: https://www.ncbi.nlm.nih.gov/geo/. GSE51588 is used for data analysis and gene screening, while GSE117999 is used as an auxiliary validation result. ROS-related genes are obtained from the Molecular Signatures Database.

Differential gene expression analysis

Use the"limma" (Linear Models for Microarray Data;3.54.0;https://bioconductor.org/packages/release/bioc/html/limma.html)package to screen differentially expressed genes (DEGs), and select DEGs with adjusted P-value < 0.05 and |log2 fold change (FC)| > 1 as the criteria. Obtain heatmaps and volcano plots of DEGs using the "ComplexHeatmap" (2.15.1;https://bioconductor.org/packages/release/bioc/html/ComplexHeatmap.html)and "ggplot2"(Grammar of Graphics;3.4.1;https://ggplot2.tidyverse.org) software packages, respectively.

WGCNA and identification of candidate genes

Perform WGCNA (weighted gene co-expression network analysis;1.72.0;https://cran.r-project.org/web/packages/WGCNA/index.html) on the merged data set to explore gene interactions and identify co-expression of genes and modules. Use hierarchical clustering based on the Euclidean distance of sample expression levels. No outlier samples were observed. Determine the soft threshold for the data, perform module partitioning, calculate the genes with the highest correlation within the modules, and compare the differentially expressed genes with the module genes using the "VennDiagram" (1.7.1;https://bioconductor.org/packages/release/bioc/html/VennDiagram.html) software. Obtain genes that are differentially expressed in OA and strongly correlated with ROS as candidate genes.

GO functional annotation and KEGG analysis

To perform Gene Ontology annotation and Kyoto Encyclopedia of Genes and Genomes (KEGG) enrichment of the candidate genes, we utilized R packages "clusterProfiler"(4.2.2;https://bioconductor.org/packages/release/bioc/html/clusterProfiler.html)[17]. GO annotation enrichment terms are determined based on biological processes (BP), cellular components (CC), and molecular functions (MF) to identify their biological characteristics. KEGG enrichment analysis is also performed to identify key signaling pathways associated with candidate genes[18–20].

PPI network construction and pathway enrichment analysis of hub genes

Using The Search Tool for the Retrieval of Interacting Genes (STRING; https://string-db.org) and Cytoscape(3.9.1;https://cytoscape.or), a protein-protein interaction (PPI) network was constructed. Then, four algorithms: 'Stress', 'BottleNeck', 'Degree', and 'EPC' were employed to screen for the hub genes within the network. The intersection of the results from these four algorithms was taken to identify hub genes. The hub genes were analyzed by Gene Set Enrichment Analysis (GSEA). |NES|>1 and FDR < 0.25 were considered as significantly enriched.

Validation of hub genes in OA

ROC curves from GSE51588 and GSE117999 datasets were used to analyze the diagnostic ROC curve analysis was used on the GSE51588 and GSE117999 datasets to evaluate the diagnostic accuracy of hub genes. Hub genes were identified using validating criteria of AUC > 0.70 and a relative expression level with $P < 0.05$ from the wilcoxTest. Further analysis of hub gene expression, combined with ROC curves and expression trends, selected hub genes with consistent expression trends and differences in both datasets to construct an artificial neural network model. The sensitivity of hub genes in diagnosing the disease was analyzed.

Measurement of immune infiltration and correlation of hub genes with immune cells

Immunological analysis was performed using the ssGSEA algorithm to analyze the differences in immune cell infiltration between OA and normal groups, as well as the correlation between hub genes and immune cells.

Chondrocyte samples

This study was approved by the Ethics Committee of Xinhua Hospital Affiliated to Dalian University. Articular cartilage samples were obtained from 2 patients with osteoarthritis who underwent knee replacement surgery. The cartilage from the diseased area of the patients was selected and labeled as the OA group. This group exhibited severe fibrosis on the cartilage surface, obvious cracks, and cartilage defect thickness greater than 50%, but the subchondral bone was not exposed. The cartilage with better morphology around the diseased area was selected and labeled as the control group. This group had normal cartilage appearance, appearing light white or slightly yellow, with no significant cracks, erosion, or ulcer formation.All cartilage samples were extracted and processed in accordance with the Helsinki Declaration. The cartilage tissue was cut into small tissue pieces with a scalpel and stored at -80 °C for freezing preservation.

Expression of the hub gene

Cartilage cells were collected from different cartilage regions of 2 OA patients for qRT-PCR detection to determine whether the expression of the screened hub genes in OA patients was consistent with the results from the datasets. Total RNA was extracted from the cartilage cells using the SYBR Green PCR kit (manufacturer: Thermo, catalog number: #K0223), and the total RNA was reverse-transcribed into cDNA using the reverse transcription kit (manufacturer: Fermentas, catalog number: #K1622). A fluorescent quantitative polymerase chain reaction (qRT-PCR) reaction system (25 μL) was constructed. GADPH was used as an internal control. The gene expression level was estimated using the $2^{-\Delta\Delta Ct}$ method.

Western blotting

The articular cartilage tissue was mixed with protein lysis buffer (manufacturer: Beyotime) and the mixture was lysed on ice (4℃) for 30 min. The supernatant was centrifuged at 12,000 rpm for 15 min, and the protein concentration was determined using the BCA method, the β-Actin was used as an internal control. SDS-PAGE gel electrophoresis was performed and the proteins were transferred to a PVDF membrane. The membrane was blocked with 5% skimmed milk for 2 h and then incubated with goat polyclonal antibody against human XOR as the primary antibody overnight. HRP-conjugated polyclonal anti-goat antibody was used as the secondary antibody for 2 h of incubation. The membrane was exposed and developed using ECL luminescent solution on a gel imaging system, and the gray value of the bands was analyzed using Image J to evaluate the expression of XDH in the cartilage.

ROS content detection

Cartilage cells were extracted from the cartilage tissue. DCFH-DA was diluted in serum-free culture medium at a ratio of 1:1000 to achieve a final concentration of 10 μM. After collection, the cells were suspended in the diluted DCFH-DA solution at a concentration of 1 to 20 million cells/mL and incubated in a cell culture incubator at 37℃ for 20 min to allow sufficient contact between the probe and the cells. The cells were washed three times with serum-free cell culture medium to thoroughly remove the DCFH-DA that did not enter the cells. Add Rosup (50 mg/ml) to the positive control well as a positive control.The cells were then placed in a microplate reader, and the fluorescence intensity was detected with an excitation wavelength of 488 nm and an emission wavelength of 525 nm.

H&E staining and immunohistochemistry

The cartilage from different area of the knee was removed and placed in 4% (w/v) paraformaldehyde for 48 h. The femoral side of the knee was then incubated in a decalcifying solution of 25% (v/w) EDTA solution (pH 7.0) at room temperature. The liquid was changed every 3 days until the femoral side of the knee was soft enough to be sectioned. The treated tissues were.

embedded in paraffin and sliced. The histological sections were stained with H&E staining.After dewaxing and hydration of the tissue sections, antigen retrieval, and removal of endogenous peroxidase, the sections were incubated with primary antibodies against MMP-13, IL-6 and COX-2 overnight at 4℃. The next day, the sections were incubated with secondary antibodies at 37℃ for 20 min, followed by visualization using a DAB solution kit. The sections were then counterstained with hematoxylin, differentiated, and blued. Images were captured under a microscope for observation.

Statistical analysis

The statistical software R version 4.2.0 was applied to perform the bioinformatics analysis, with p-values of < 0.05 suggesting statistical significance. The GraphPad Prism 6.0 software (GraphPad Prism) was used to analyze

cartilage samples data. All data are expressed as the mean ± standard error of the mean (SEM), and $p < 0.05$ was considered significant.

Results

Identification of DEGs and candidate genes

A total of 6472 DEGs between OA and normal groups were screened from the GSE51588 dataset, including 3974 upregulated genes and 2498 downregulated genes. The volcano plot and heatmap revealing the clustering relationship between OA and normal group samples are shown in Fig. 1(a) and Fig. 1(b), respectively. Next, we performed ssGSEA scoring for ROS-related genes, and the results are shown in Fig. 2(a), indicating a difference between the two groups. This suggests a correlation between ROS-related genes and OA. Subsequently, we conducted WGCNA analysis based on the scores. Initially, we used Euclidean distance of sample expression levels for hierarchical clustering, and the results showed no outlier samples (Fig. 2(b)), allowing us to proceed with subsequent analyses. In our study, we selected a power of β = 12 (scale-free R2 = 0.9) as the soft threshold to ensure a scale-free network (Fig. 2(c)). A total of 7 modules were obtained that exhibited similar co-expression patterns among these genes (Fig. 2(d)). The module genes in the green module (*r*=-0.82; P = lc-05) were significantly correlated with OA (Fig. 2(e)), containing 2570 module genes. By intersecting the screened differential genes with the module genes in the green module, we obtained 698 candidate genes (Fig. 2(f)).

Functional enrichment analyses of the intersection genes

With the purpose of investigating the biological activities associated with FDEGs among the OA cases, the GO and KEGG enrichment analyses were performed on the 698 genes. In the GO analysis of candidate genes, the enriched BP terms were regulation of postsynaptic membrane potential, positive regulation of natural killer cell mediated immunity, and regulation of natural killer cell mediated immunity; the enriched CC terms were GABA-A receptor complex, GABA receptor complex, and chloride channel complex; the enriched MF terms were extracellular ligand-gated monoatomic ion channel activity, ligand-gated monoatomic anion channel activity, and transmitter-gated monoatomic ion channel activity (Fig. 3(a)). KEGG enrichment analysis showed that these genes were significantly enriched in Nicotine addiction, Neuroactive ligand-receptor interaction, Antigen processing and presentation and other pathways. (Fig. 3(b)).

Construction of PPI and pathway enrichment analysis of hub genes

The protein network interaction map composed of 698 candidate genes is shown in Fig. 4(a). The core genes in the network were screened through four algorithms: 'Stress', 'BottleNeck', 'Degree', and 'EPC'. The intersection of the four algorithms yielded five hub genes: ALB, CDH1, HSPA8, HIST1H2BE, and XDH (Fig. 4(b)). Then, gene set enrichment analysis (GSEA) was performed on the five selected hub genes, and |NES|>1 and FDR < 0.25 were considered as significant enrichment. Among them, the XDH gene was accurately enriched in the ROS pathway (Fig. 4(c)).

Identification of the hub genes

To further confirm the expression levels and disease prediction capabilities of the selected hub genes, we performed validation in another dataset, GSE117999. The results showed that the five hub genes exhibited

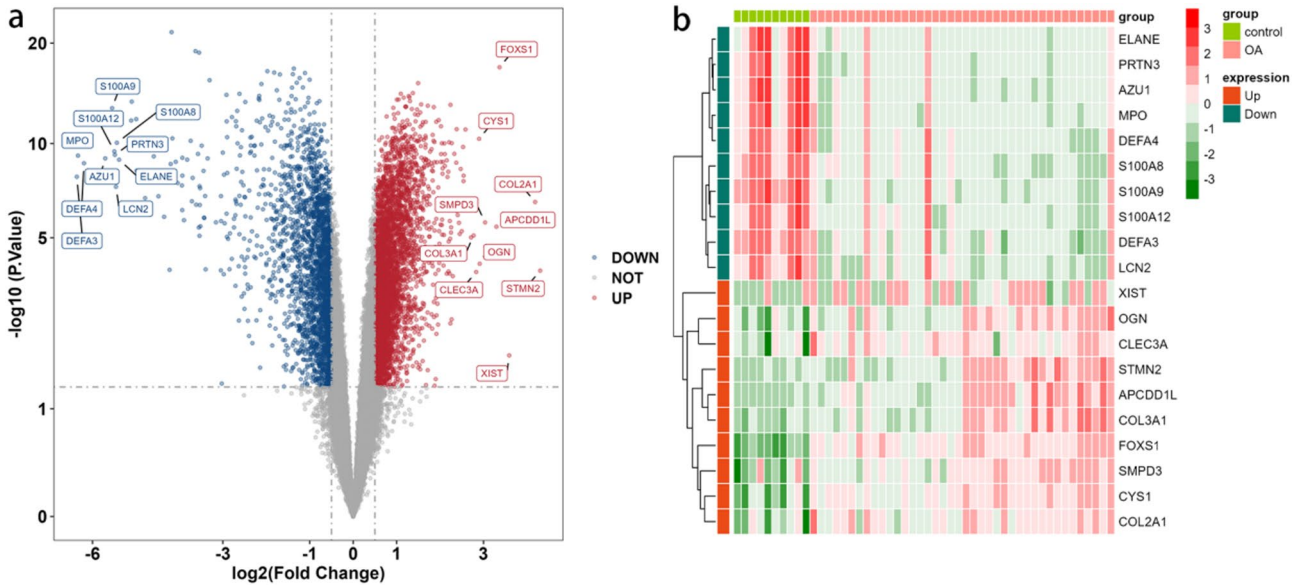

Fig. 1. Volcano plot and heatmap of DEGs identified from the integrated dataset: (a) Red dots represent upregulated genes, while blue dots represent downregulated genes; (b) Each row in the heatmap represents a DEG, and each column represents a sample.

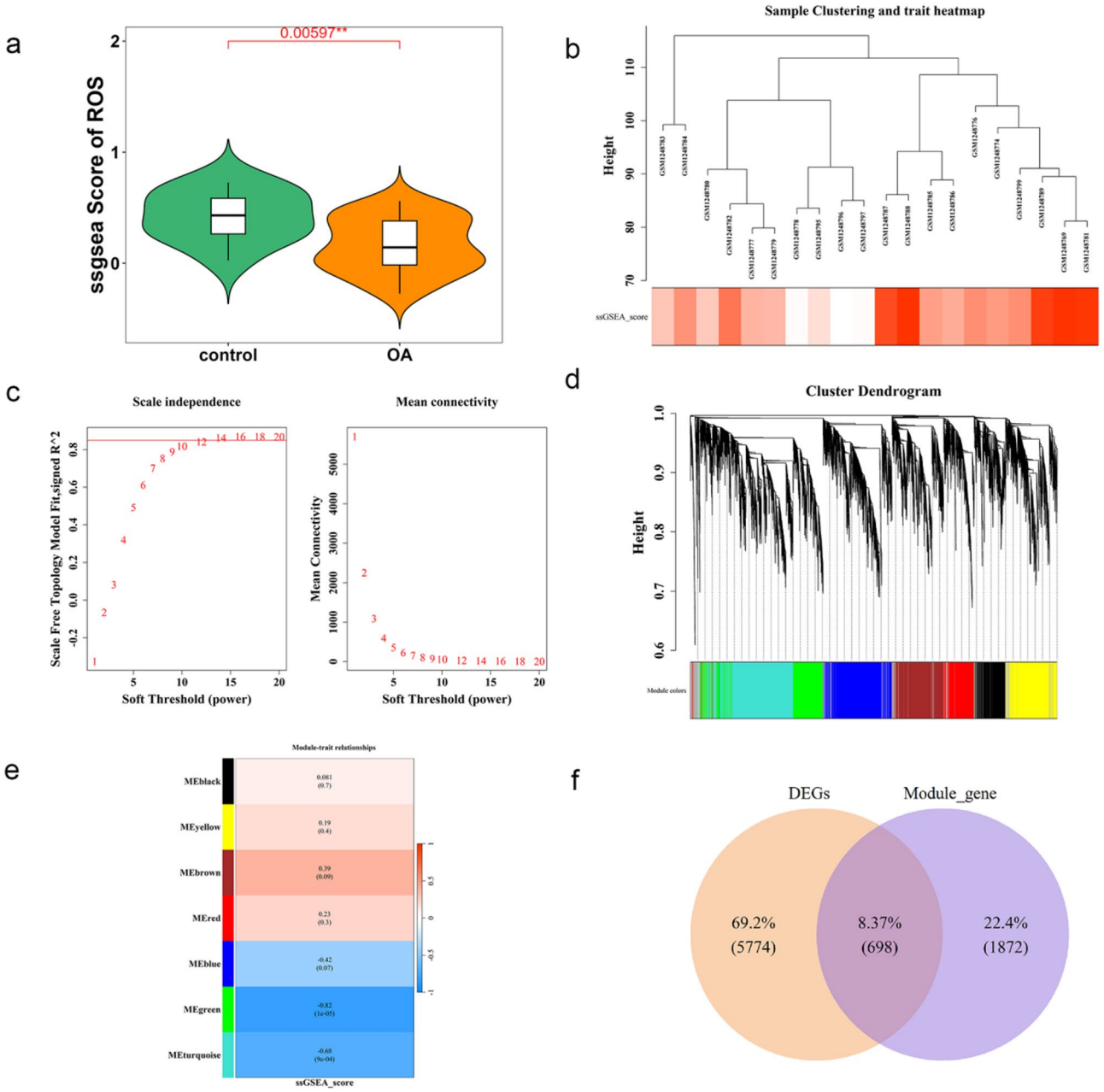

Fig. 2. Screening candidate genes using WGCNA analysis and "VennDiagram" software: (a) Conduct ssGSEA scoring on ROS genes to determine inter-group differences; (b) Perform hierarchical clustering based on the Euclidean distance of sample expression levels to identify outlier samples; (c) Determine the optimal soft threshold; (d) Gene co-expression modules, with each color representing a co-expression module; (e) Heatmap of module-OA associations; the green module shows the strongest correlation; (f) Venn diagram of the overlap between DEGs and module genes in the green module.(**$P < 0.01$).

relatively good predictive ability (Fig. 5(a-b)), among which the three gene groups of ALB, HIST1H2BE, and XDH showed the same expression trends in both datasets (Fig. 5(c-d)). An artificial neural network was constructed for these three gene groups (Fig. 6(a-d)), and the results showed that the three gene groups could effectively distinguish OA and the control group, demonstrating high sensitivity in disease diagnosis.

Analysis of immune infiltration

Using the ssGSEA algorithm, we identified ten types of immune cells that showed differential expression between OA and normal groups (Fig. 7(a)).Subsequently, we conducted a study on the correlation between immune cells and immune cells (Fig. 7(b)), and between hub genes and immune cells (Fig. 7(c)).Combining the results of these two studies, we found that the immune cells with high correlation to the XDH gene include activated dendritic cells, central memory CD4 T cells, effector memory CD4 T cells, immature dendritic cells,

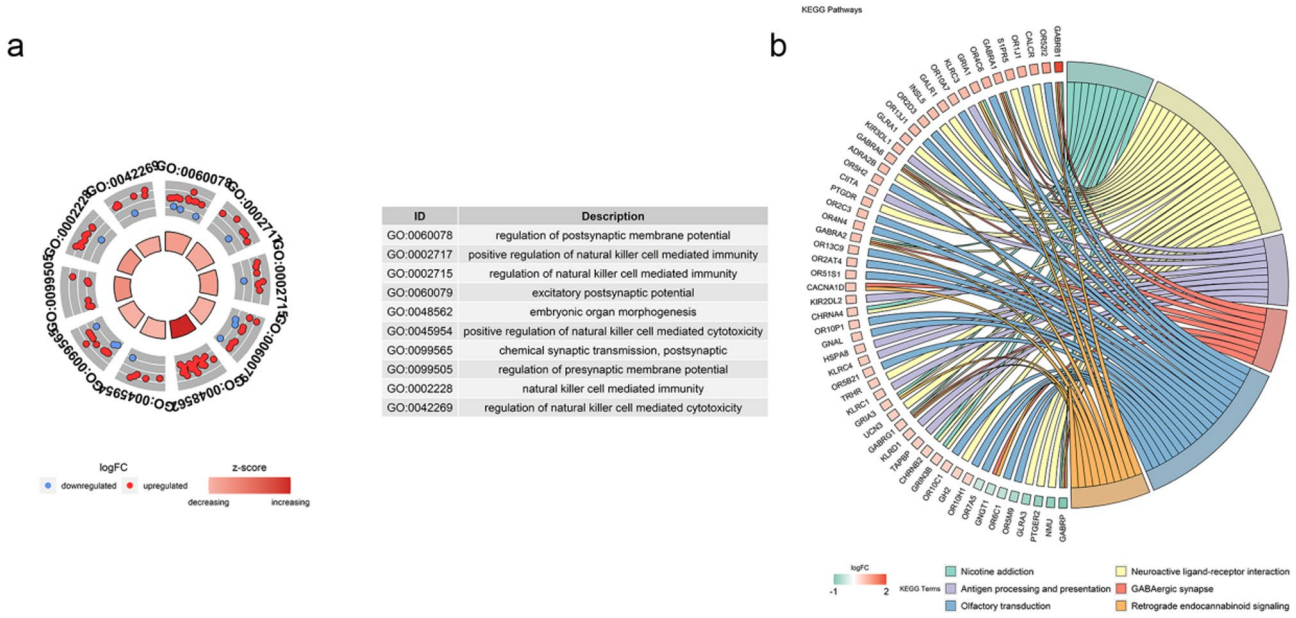

ID	Description
GO:0060078	regulation of postsynaptic membrane potential
GO:0002717	positive regulation of natural killer cell mediated immunity
GO:0002715	regulation of natural killer cell mediated immunity
GO:0060079	excitatory postsynaptic potential
GO:0048562	embryonic organ morphogenesis
GO:0045954	positive regulation of natural killer cell mediated cytotoxicity
GO:0099565	chemical synaptic transmission, postsynaptic
GO:0099505	regulation of presynaptic membrane potential
GO:0002228	natural killer cell mediated immunity
GO:0042269	regulation of natural killer cell mediated cytotoxicity

Fig. 3. Functional enrichment analysis of candidate genes: (a) GO analysis of candidate genes; (b) KEGG analysis of candidate genes.

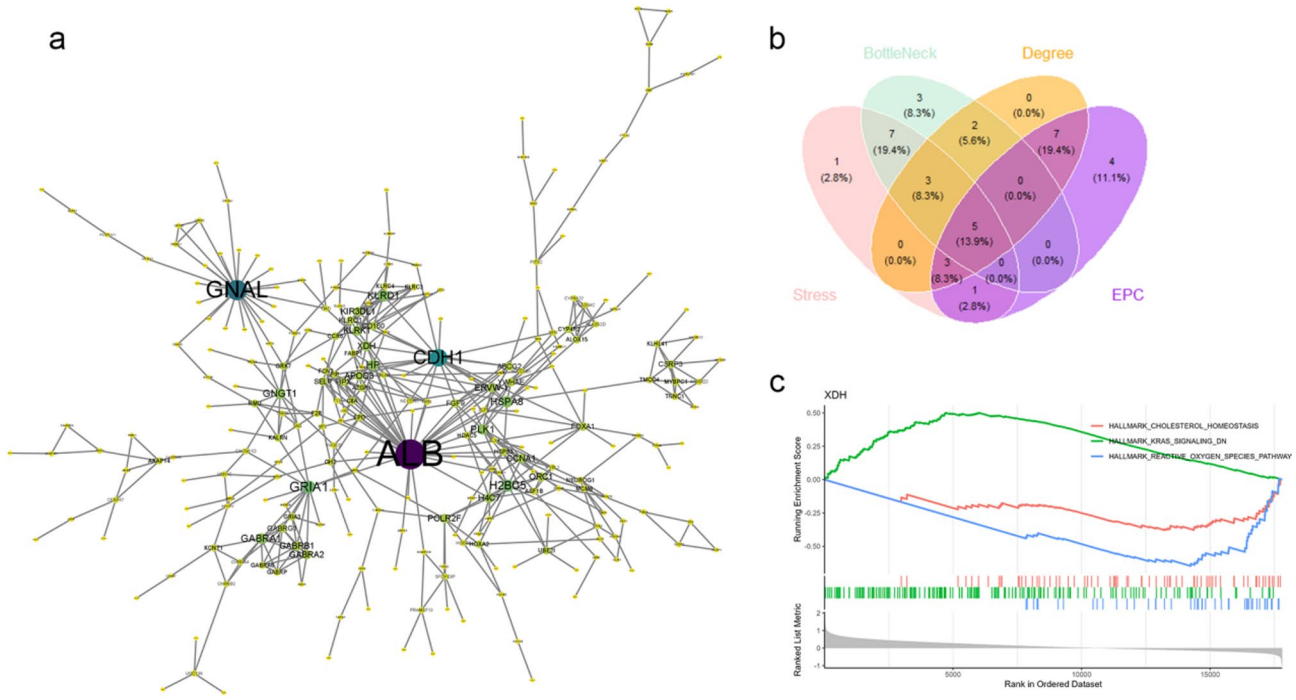

Fig. 4. Hub gene selection and pathway functional enrichment analysis: (a) Protein-protein interaction (PPI) network diagram; (b) Four algorithms: 'Stress', 'BottleNeck', 'Degree', and 'EPC' are used to screen the core genes in the network, and the intersection of these four algorithms yields 5 hub genes; (c) GSEA analysis of the XDH gene, where the blue line indicates that the XDH gene can accurately enrich in the ROS pathway.

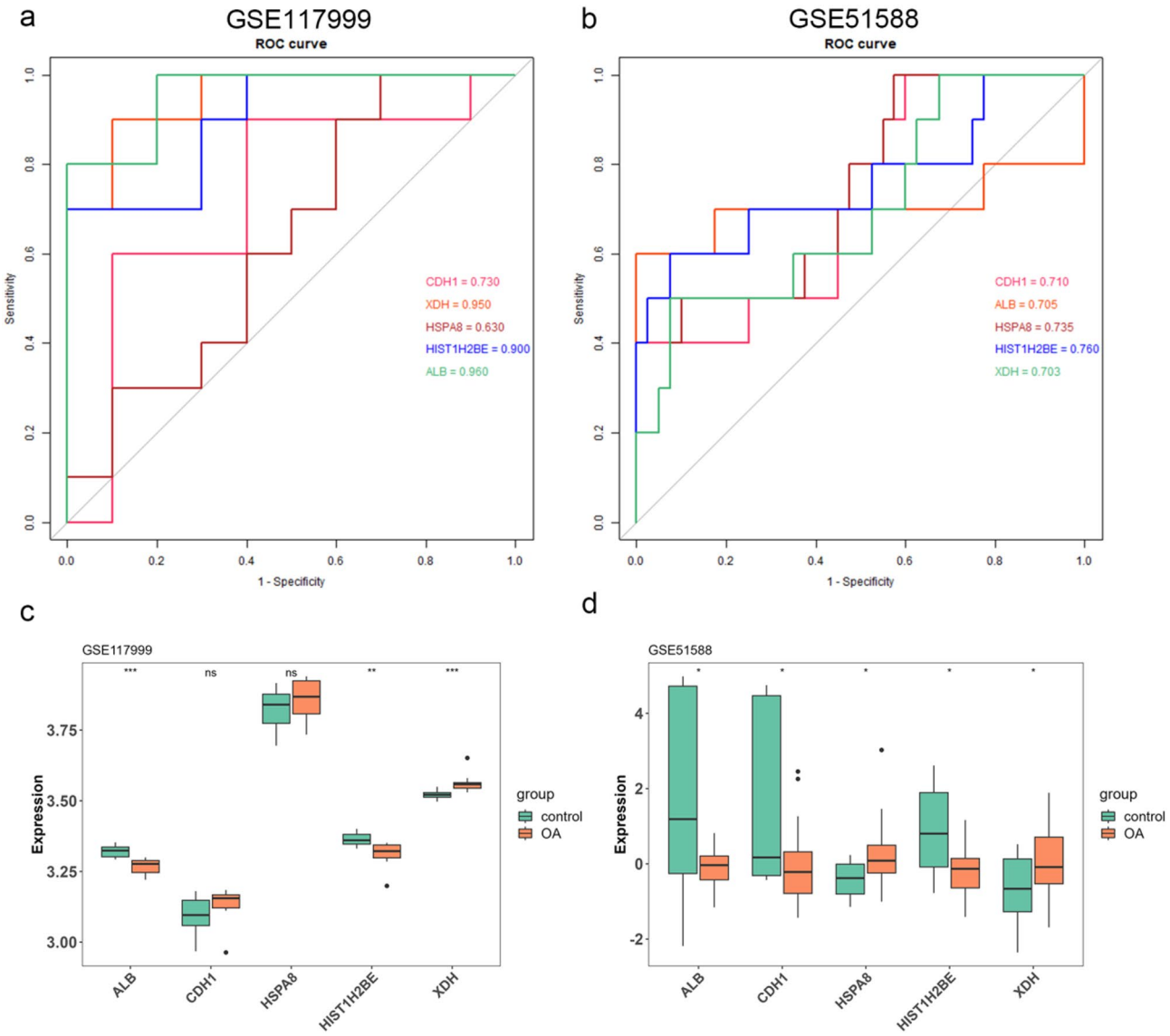

Fig. 5. ROC curves and expression levels of hub genes.: (a-b) The ROC curves demonstrate the predictive performance of each hub gene, where AUC (Area Under the Curve) > 0.7 indicates a diagnostic value with some reference significance; (c-d) Box plots showing the differences in hub gene expression levels between the OA group and the control group.(*$P < 0.05$,**$P < 0.01$,*** $P < 0.001$,ns $P > 0.05$).

macrophages, MDSCs, monocytes, and plasmacytoid dendritic cells. For the HIST1H2BE gene, the immune cells with high correlation are activated dendritic cells, activated CD4 T cells, macrophages, and neutrophils. No immune cells showed high correlation with the ALB gene.

XDH gene expression and ROS content detection in OA

Since the XDH gene can be well enriched in the ROS pathway and exhibits good disease prediction ability and diagnostic sensitivity, we selected the XDH gene for mRNA and protein expression level detection. The qRT-PCR and Western Blotting (WB) test were used to detect the relative expression of XDH in OA and healthy chondrocytes. The WB results showed that the protein expression level of XDH in the OA group was increased compared to the control group (Fig. 8(a)-8(b)). Meanwhile, the mRNA expression of XHD in OA chondrocytes was significantly upregulated than that in control chondrocytes (Fig. 8(c)). In addition, The ROS content in OA and normal control chondrocytes was detected using the fluorescent probe DCFH-DA technology, and the results showed that the ROS content in OA chondrocytes was significantly increased compared to control chondrocytes (Fig. 8(d)).

Histology and immunohistochemistry

The degree of OA was evaluated using H&E staining related to the smoothness of the articular cartilage surface, the distribution of chondrocytes, and the integrality of osteochondral junction.Results were showed in Fig. 9

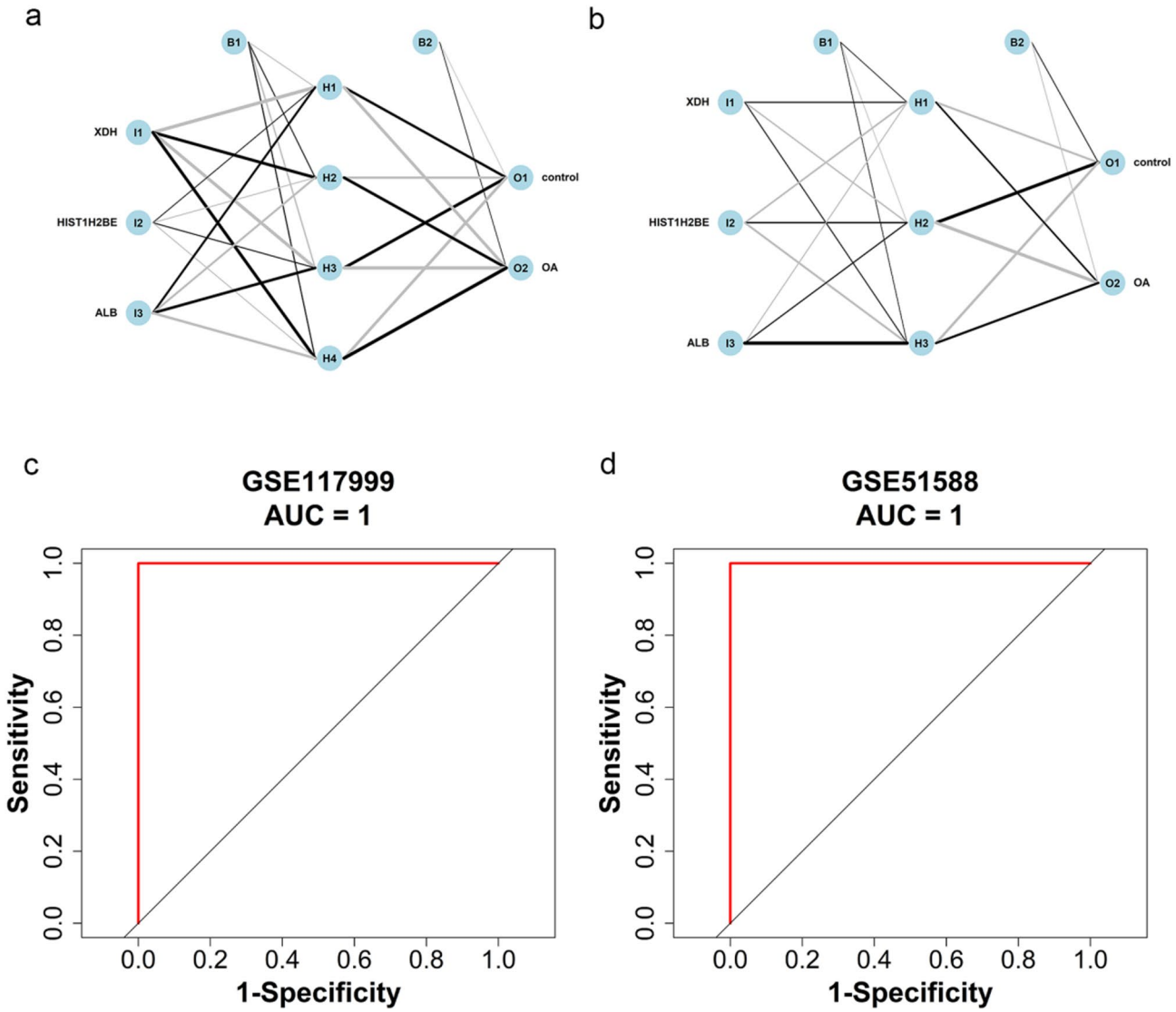

Fig. 6. Disease diagnostic capability of hub genes: (a-b) Artificial neural network diagrams of hub genes; (c-d) ROC curves, where AUC (Area Under the Curve) > 0.9 represents a good model differentiation effect.

.In OA group, the surface of the articular cartilage was destroyed. The chondrocytes were disorganized, a cavity had formed between the connection of the cartilage and bone, and fibrocartilage was formed on the surface of the cartilage. In normal group, the surface of the articular cartilage was layered with disorganized chondrocytes and there was an intact osteochondral connection. The inflammation-related factors were detected by immunohistochemical test in OA and normal cartilage tissue and results were showed in Fig. 9. The results showed that the staining of MMP-13, IL-6 and COX-2 was significantly higher in OA cartilage tissue than that in control group, Meanwhile, the number of brown bodies in OA chondrocytes was significantly more than that in healthy cartilage. Therefore, we can conclude that the inflammatory response in OA cartilage is significantly higher than that in the control group.

Discussion

It is well known that ROS mediated oxidative stress plays an important role in the pathogenesis of OA. In current study, a total of 698 genes related to both ROS and OA were screened and subjected to functional enrichment analysis. GO enrichment analysis revealed that these genes are mainly enriched in biological processes such as innate immune regulation mediated by natural killer cells and participate in molecular functions such as major histocompatibility complex (MHC) protein complex binding. KEGG enrichment analysis results showed that the genes are related to antigen processing and presentation. MHC molecules are key molecules for the immune system to recognize "self" and "non-self". They are responsible for presenting antigenic peptides on the cell surface for recognition by T cells. Antigen processing and presentation is a crucial process in the immune system, involving the uptake and processing of antigens by antigen-presenting cells (APCs) and their presentation on the

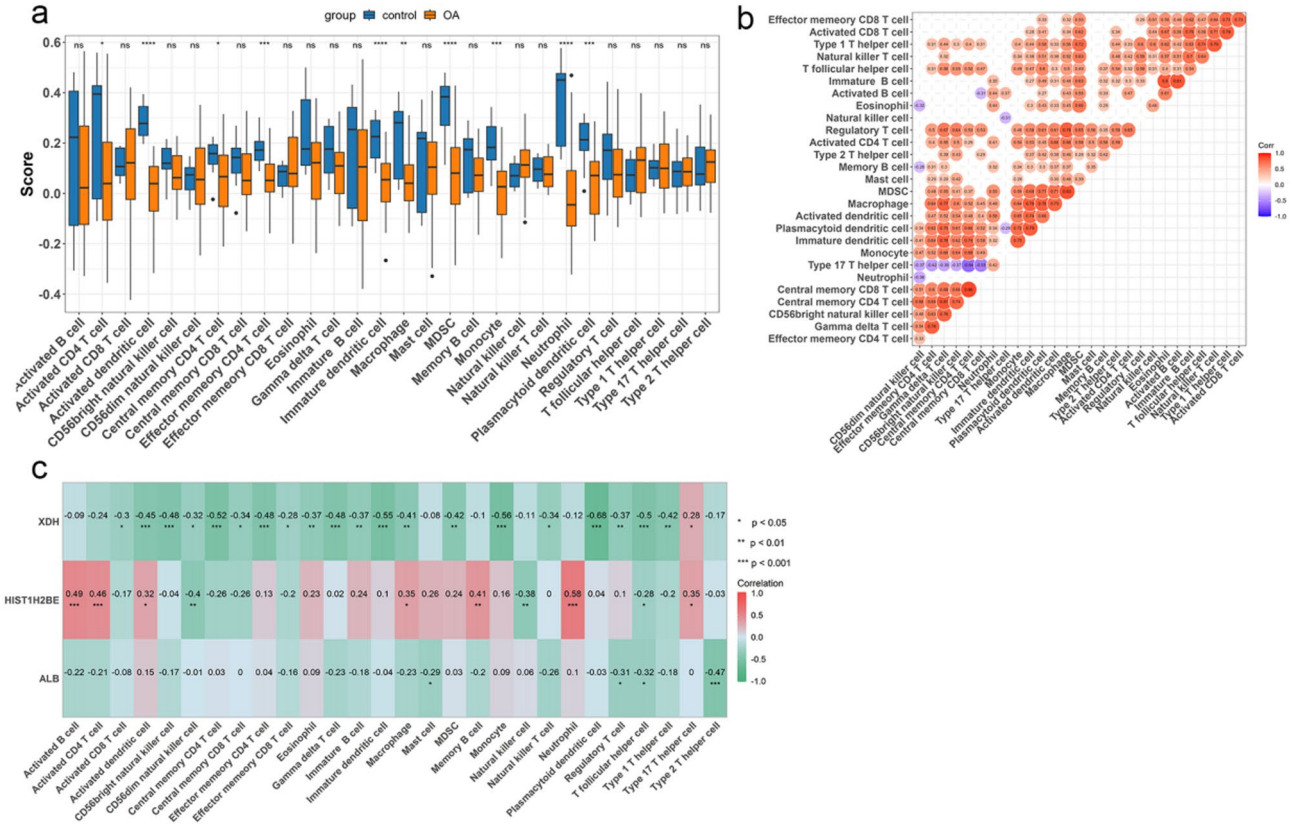

Fig. 7. Analysis of immune infiltration between OA and control groups: (a) Using the ssGSEA algorithm to detect cells with differences between the disease and control groups; (b) Correlation between immune cells; (c) Correlation between hub genes and immune cells.(*$P<0.05$,**$P<0.01$,*** $P<0.001$,ns $P>0.05$).

cell surface in the form of immunogenic peptides, ultimately recognized by immune-active cells such as T cells. These results indicate the important role of ROS and OA-related genes in immune regulation.

Through bioinformatics analysis, we successfully identified three hub genes (ALB, HIST1H2BE and XDH) from 698 genes, all of which have strong correlations with OA and ROS. Among them, the ALB and HIST1H2BE genes are downregulated in the OA group, while the XDH gene is upregulated. More importantly, the XDH gene can be accurately enriched in the ROS pathway. The transcription product of the XDH gene is xanthine oxidoreductase (XOR), an enzyme containing molybdenum and iron proteins involved in oxidative metabolism. It is well known that XOR is an enzyme present in two interconvertible forms, xanthine dehydrogenase (XDH) and xanthine oxidase (XO)[21], both of which participate in uric acid formation and are related to ROS production[22,23]. Experimental studies confirm XOR's critical role in chondrocyte mineralization and OA progression: XOR inhibitors (febuxostat, allopurinol) reduce CPP-induced mineralization and IL-6 secretion; CRISPR/Cas9 XOR knockout in ATDC5 cells decreases mineralization, Alp activity, and ROS generation under HA stimulation. XO-form (XO ki) murine chondrocytes exhibit stronger mineralization, higher Alp/IL-6, and reduced GAG (ECM marker) versus XDH-form cells. Clinically, OA-damaged human cartilage shows upregulated XOR expression, co-localized with calcium crystals and elevated IL-6, paralleling increased ROS levels. These findings link XOR to OA pathology via promoting mineralization, inflammation, and ECM damage[24].

The activity of XOR is also closely related to nitrite (NO_2-) and NO metabolism in the body. When XOR is expressed as XDH, xanthine is oxidized to uric acid, and electrons are transferred to FAD through two Fe/S centers. In FAD, NAD + is reduced to NADH, and under the catalysis of NADH oxidase (NOX), ROS and NO are produced[25]. When expressed as XO, it can act as an electron acceptor for oxygen molecules, it reduces NO_2- to NO while NADH is reduced to NAD+, directly producing O_2- and H_2O_2[26]. These NO and O_2- can react to derive reactive nitrogen species (RNS) and peroxynitrite (ONOO-), which further induce protein and lipid nitrosation, generating a large amount of lipid peroxides (LPO) and nitrosylated products. This leads to an imbalance in the redox homeostasis of the synovial membrane, thereby causing a series of OA pathological changes such as synovial hyperplasia and degeneration, and pannus formation[27]. On the other hand, XOR mainly catalyzes the conversion of inosine to xanthine and then to uric acid, with simultaneous production of ROS[28]. Some studys had demonstrated the correlation between uric acid concentration in the blood or the synovial fluid and OA incidence[29]. A cohort study showed a positive correlation between the uric acid concentration in the synovial fluid and IL-1 or IL-18 concentration, and these concentrations showed positive correlation with progression of knee OA[30]. In a study comprised of patients who received artificial joint operations for the hip or knee joints, a correlation was observed between the onset of systemic OA and uric acid levels in the blood[31]. In this study,

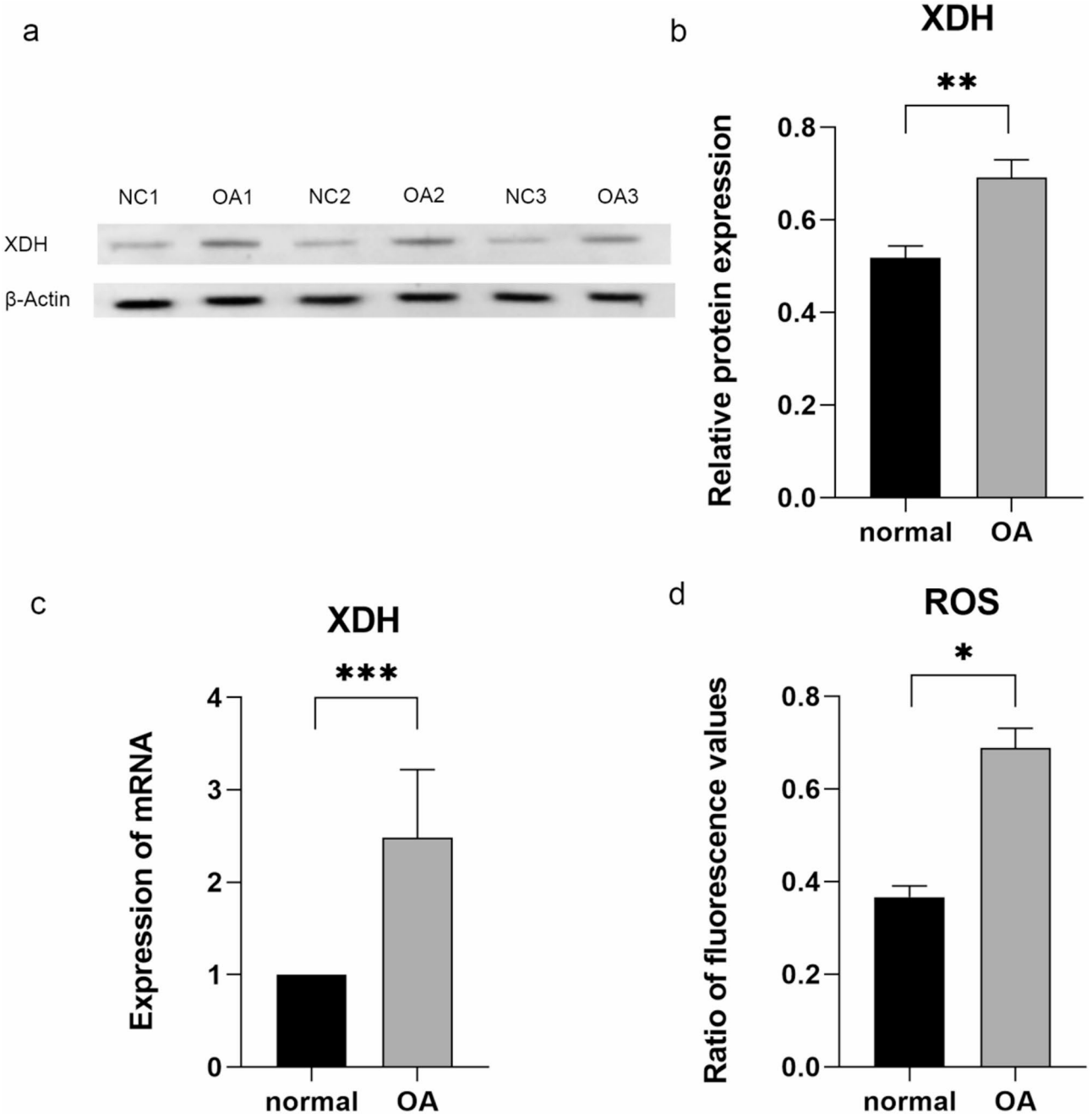

Fig. 8. qRT-PCR and WB validation of XDH gene expression and ROS content detection between OA and control chondrocytes: (a-b) WB detection and quantitative analysis show the XDH protein level in chondrocytes.The blank areas in Figure a represent the stitching regions of different gel images. The complete original images can be found in the Supplementary file; (c) Relative mRNA expression level of the XDH gene was calculated using the $2^{-\Delta\Delta Ct}$ method.;(d) ROS content was detected using a fluorometer. (*$P<0.05$,**$P<0.01$,*** $P<0.001$).

the XDH gene was significantly upregulated in the OA group in both gene pools, indicating that under OA conditions, the upregulated expression of the XDH gene generates xanthine dehydrogenase (XDH) and xanthine oxidase (XO), which subsequently produce excessive ROS, leading to oxidative stress to induce or aggravate the pathological degree of OA.

At last, we used the ssGSEA algorithm to verify the infiltration of immune cells in OA synovial membranes and the correlation between the XDH gene and immune cells. The results showed significant differences in some immune cells between the OA group and the normal group. Eight types of immune cells had a high correlation with the XDH gene.These correlations are biologically relevant to OA pathology and bridge XOR-mediated oxidative stress with immune responses.Activated DCs (aDCs) likely recognize XOR/ROS-induced damage-

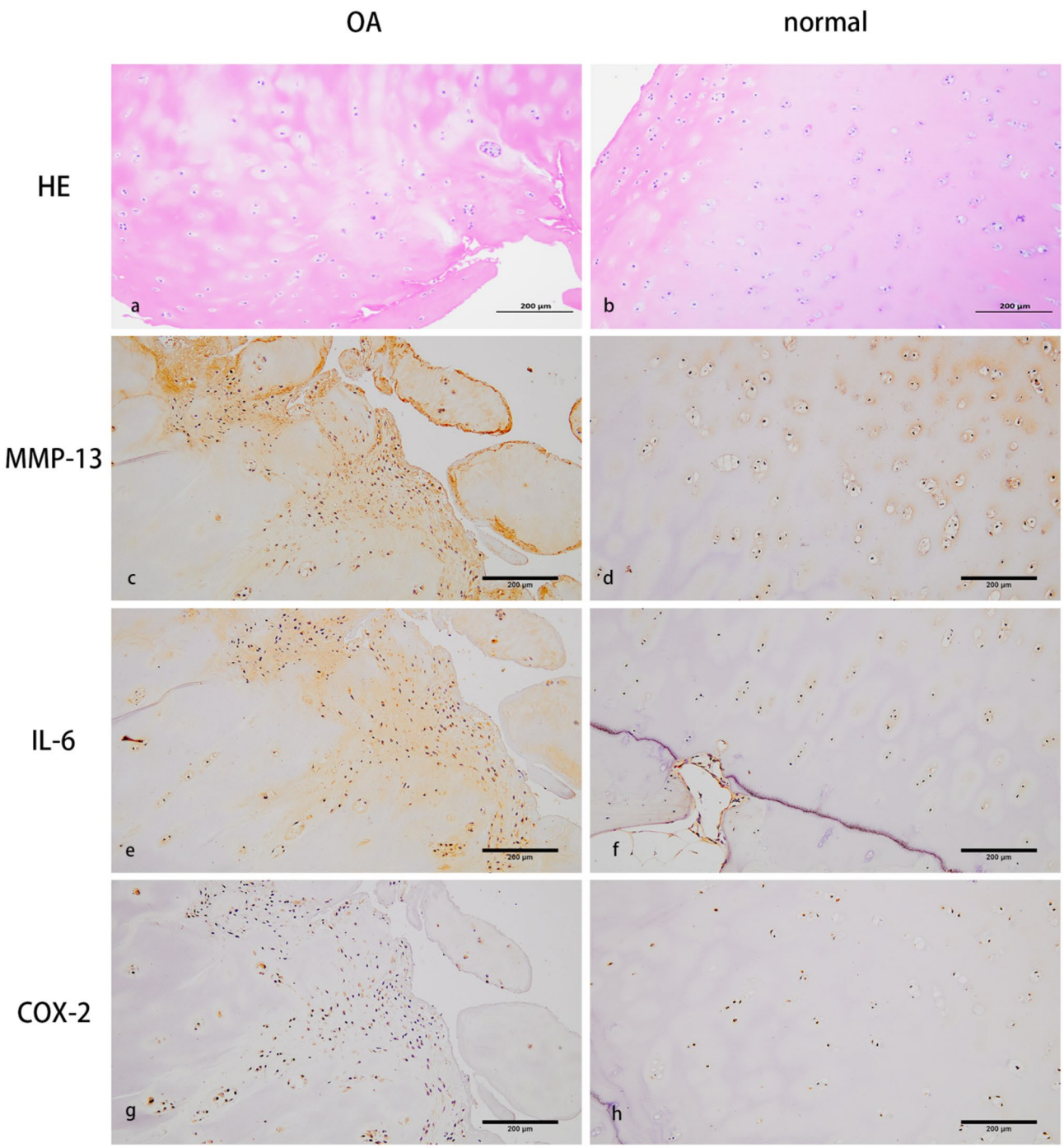

Fig. 9. a: HE staining in the OA group (×100); b: HE staining in the normal group (×100); c: MMP-13 expression in the OA group (×100); d: MMP-13 expression in the normal group (×100); e: IL-6 expression in the OA group (×100); f: IL-6 expression in the normal group (×100); g: COX-2 expression in the OA group (×100); h: COX-2 expression in the normal group (×100).

associated molecular patterns (DAMPs) from degenerating chondrocytes, such as oxidized extracellular matrix (ECM) components or uric acid crystals[32]. They present these DAMPs to T cells via MHC molecules, initiating adaptive immune responses. Immature DCs (iDCs), under ROS stimulation, may mature into aDCs, amplifying T cell activation and sustaining chronic inflammation[33].Central memory (Tcm CD4+) and effector memory (Tem CD4+) T cells, once primed by aDCs, rapidly secrete pro-inflammatory cytokines (e.g., IL-6, IFN-γ) upon re-encountering antigens[34]. XOR-mediated ROS may enhance their proliferation and effector function, exacerbating local inflammation and cartilage degradation[35].As key innate immune cells, macrophages are highly responsive to ROS. Under XOR-induced oxidative stress, they polarize to pro-inflammatory M1 phenotypes, releasing IL-1β, TNF-α, and other factors that synergize with XOR-upregulated IL-6 to form a feedforward loop:

pro-inflammatory cytokines further increase ROS production and matrix metalloproteinase (MMP) expression, accelerating ECM degradation[36].These findings fully indicate that oxidative stress induced by XOR-mediated ROS (transcribed by the XDH gene) may be a key factor in the pathogenesis of OA, linking innate and adaptive immune responses to drive joint damage.

Meanwhile, we collected damaged and normal cartilage from patients undergoing total knee arthroplasty (TKA) to further test this hypothesis. Firstly, an immunohistochemical analysis of human cartilage samples was performed to assess the inflammatory response within the OA cartilage. The results showed that the levels of MMP-13, IL-6 and COX-2 in chondrocytes in the OA group were significantly increased compared with those in the control group, indicating a clear inflammatory response in the OA chondrocytes. Studies have shown that excessive ROS can exacerbate joint cartilage calcification and damage by upregulating the expression of metalloproteinases (MMPs), triggering inflammatory responses, promoting the expression of cytokines such as IL-6 and COX-2, and activating the NF-κB and MEK/ERK signaling pathways to induce inflammatory responses[10,37,38]. Multiple studies have shown that NO and $ONOO^-$ can activate and increase the activity of COX-2[39,40], thereby inducing premature aging of articular chondrocytes[41]. Subsequently, we used qRT-PCR and Western blotting (WB) techniques to detect XDH gene and protein expression in the sample cartilage. The results showed that XDH gene and its transcription protein were highly expressed in the cartilage of OA patients, which further confirmed the strong correlation between XDH gene and its transcription products and OA. Meanwhile, we also found that the ROS content in damaged cartilage was significantly higher than that in normal cartilage, indicating that there were a large number of ROS in damaged cartilage of OA patients. This also suggests that XDH gene and its transcriptional protein XOR are closely related to the occurrence and development of OA in ROS-mediated oxidative stress.

In summary, this study identified the XDH gene as a key gene for ROS-mediated oxidative stress in osteoarthritis pathology and confirmed its specific expression in chondrocytes, which may contribute to our understanding of the progression of osteoarthritis and provide prognostic biomarkers and therapeutic targets. However, our study also has certain limitations. Firstly, GAPDH was used as the reference gene for qPCR in this study. However, previous literature (Zhang Z et al., PLoS One, 2013) has indicated its expression may be unstable during chondrogenic differentiation or under pathological conditions, potentially affecting quantitative accuracy. Due to sample exhaustion and time constraints, we were unable to replace it with more stable reference genes (e.g., HPRT, PPIA) or follow GLP guidelines to validate results using multiple reference genes. Secondly, While we validated the immunological characteristics of the samples via pro-inflammatory factors (e.g., IL-6), we did not perform co-localization staining of XDH with immune cells (e.g., macrophages, dendritic cells) due to tissue preservation volume and antibody limitations. The association between XDH and immune cell infiltration was inferred solely from statistical correlations, lacking direct histological evidence. Future studies will focus on the following improvements:

1. Adopt stable reference genes (e.g., HPRT, PPIA) and implement multi-reference gene normalization as per GLP guidelines;
2. Expand the sample size ($n \geq 20$) and supplement co-staining experiments of XDH with immune cell markers;
3. Validate the causal role of XDH through in vitro/in vivo functional experiments (e.g., overexpression/knockdown, gene knockout mice).

Conclusions

Bioinformatics and experimental data showed that compared with the control group, XDH gene serves as a pivotal gene in ROS-mediated oxidative stress in OA pathology. Our study may provide a new pivotal gene for ROS-mediated oxidative stress, which has potential clinical applications in the pathology, diagnosis, and treatment of OA.

Data availability

The datasets used and/or analyzed during the current study are available from the corresponding author on reasonable request.

Received: 25 February 2025; Accepted: 11 July 2025
Published online: 13 August 2025

References

1. Cao, F. et al. Trends and cross-country inequalities in the global burden of osteoarthritis, 1990–2019: A population-based study. *Ageing Res. Rev.* **99**, 102382 (2024).
2. Scheuing, W. J., Reginato, A. M., Deeb, M. & Acer Kasman, S. The burden of osteoarthritis: is it a rising problem? *Best Pract. Res. Clin. Rheumatol.* **37** (2), 101836 (2023).
3. Yao, Q. et al. Osteoarthritis: pathogenic signaling pathways and therapeutic targets. *Signal. Transduct. Target. Ther.* **8** (1), 56 (2023).
4. Yan, R. et al. ROS-Induced endothelial dysfunction in the pathogenesis of atherosclerosis. *Aging Dis.* (2024).
5. Wang, K. et al. Effects of REDOX in Regulating and Treatment of Metabolic and Inflammatory Cardiovascular Diseases. Oxid Med Cell Longev. ; 2020:5860356. (2020).
6. Pantea Stoian, A. et al. Oxidative stress applied in Diabetes Mellitus-A new paradigm. Proceedings ; 11, 1007. (2019).
7. Degtyareva, N. P. et al. Mutational signatures of redox stress in yeast single-strand DNA and of aging in human mitochondrial DNA share a common feature. *PLoS Biol.* **17** (5), e3000263 (2019).
8. Mittal, M., Siddiqui, M. R., Tran, K., Reddy, S. P. & Malik, A. B. Reactive oxygen species in inflammation and tissue injury. *Antioxid. Redox Signal.* **20** (7), 1126–1167 (2014).
9. Terkeltaub, R., Johnson, K., Murphy, A. & Ghosh, S. Invited review: the mitochondrion in osteoarthritis. *Mitochondrion* **1** (4), 301–319 (2002).

10. Lepetsos, P. & Papavassiliou, A. G. ROS/oxidative stress signaling in osteoarthritis. *Biochim. Biophys. Acta*. **1862** (4), 576–591 (2016).
11. Tudorachi, N. B. et al. The implication of reactive oxygen species and antioxidants in knee osteoarthritis. *Antioxid. (Basel)*. **10** (6), 985 (2021).
12. Liu, L. et al. The physiological metabolite α-ketoglutarate ameliorates osteoarthritis by regulating mitophagy and oxidative stress. *Redox Biol.* **62**, 102663. https://doi.org/10.1016/j.redox.2023.102663 (2023).
13. Yu, S. M. & Kim, S. J. Withaferin A-caused production of intracellular reactive oxygen species modulates apoptosis via PI3K/Akt and JNKinase in rabbit articular chondrocytes. *J. Korean Med. Sci.* **29** (8), 1042–1053 (2014).
14. Yu, S. M. & Kim, S. J. The thymoquinone-induced production of reactive oxygen species promotes dedifferentiation through the ERK pathway and inflammation through the p38 and PI3K pathways in rabbit articular chondrocytes. *Int. J. Mol. Med.* **35** (2), 325–332 (2015).
15. Peng, H. Y. et al. Metabolic reprogramming and reactive oxygen species in T cell immunity. *Front. Immunol.* **12**, 652687 (2021).
16. Ansari, M. Y., Ahmad, N. & Haqqi, T. M. Oxidative stress and inflammation in osteoarthritis pathogenesis: role of polyphenols. *Biomed. Pharmacother*. **129**, 110452 (2020).
17. Davies, J. M. S. et al. The oxygen paradox, the French paradox, and age-related diseases. *Geroscience* **39** (5–6), 499–550 (2017).
18. Kanehisa, M., Furumichi, M., Sato, Y., Matsuura, Y. & Ishiguro-Watanabe, M. KEGG: biological systems database as a model of the real world. *Nucleic Acids Res.* **53**, D672–D677 (2025).
19. Kanehisa, M. Toward Understanding the origin and evolution of cellular organisms. *Protein Sci.* **28**, 1947–1951 (2019).
20. Kanehisa, M. & Goto, S. KEGG: Kyoto encyclopedia of genes and genomes. *Nucleic Acids Res.* **28**, 27–30 (2000).
21. Veljković, A. et al. Xanthine oxidase/dehydrogenase activity as a source of oxidative stress in prostate Cancer tissue. *Diagnostics (Basel)*. **10** (9), 668 (2020).
22. Berry, C. E. & Hare, J. M. Xanthine oxidoreductase and cardiovascular disease: molecular mechanisms and pathophysiological implications. *J. Physiol.* **555** (Pt 3), 589–606 (2004).
23. Wu, B. et al. Association between Xanthine dehydrogenase Tag single nucleotide polymorphisms and essential hypertension. *Mol. Med. Rep.* **12** (4), 5685–5690 (2015).
24. Nasi, S. et al. Xanthine oxidoreductase is involved in chondrocyte mineralization and expressed in Osteoarthritic damaged cartilage. *Front. Cell. Dev. Biol.* **9**, 612440 (2021).
25. Battelli, M. G., Bortolotti, M., Bolognesi, A. & Polito, L. Pro-Aging effects of Xanthine oxidoreductase products. *Antioxid. (Basel)*. **9** (9), 839 (2020).
26. Ansari, M. Y., Khan, N. M., Ahmad, I. & Haqqi, T. M. Parkin clearance of dysfunctional mitochondria regulates ROS levels and increases survival of human chondrocytes. *Osteoarthr. Cartil.* **26** (8), 1087–1097 (2018).
27. Zhang, X. et al. Lipid peroxidation in osteoarthritis: focusing on 4-hydroxynonenal, malondialdehyde, and ferroptosis. *Cell. Death Discov*. **9** (1), 320 (2023).
28. Camici, M., Micheli, V., Ipata, P. L. & Tozzi, M. G. Pediatric neurological syndromes and inborn errors of purine metabolism. *Neurochem Int.* **56** (3), 367–378 (2010).
29. Aibibula, Z. et al. Xanthine oxidoreductase activation is implicated in the onset of metabolic arthritis. *Biochem. Biophys. Res. Commun.* **472** (1), 26–32 (2016).
30. Denoble, A. E. et al. Uric acid is a danger signal of increasing risk for osteoarthritis through inflammasome activation. *Proc. Natl. Acad. Sci. U S A*. **108** (5), 2088–2093 (2011).
31. Altay, M. A. et al. Evaluation of prolidase activity and oxidative status in patients with knee osteoarthritis: relationships with radiographic severity and clinical parameters. *Rheumatol. Int.* **35** (10), 1725–1731 (2015).
32. Martel-Pelletier, J. et al. Dendritic cells in osteoarthritis: potential role in the immune response. *Arthritis Res. Ther.* **12** (6), R206 (2010).
33. Kalsi, P. et al. Reactive oxygen species drive dendritic cell maturation in osteoarthritis. *Free Radic Biol. Med.* **123**, 1–11 (2018).
34. Seddon, B. et al. Central and effector memory T cells in chronic inflammation: implications for osteoarthritis. *Immunol. Rev.* **265** (1), 152–167 (2015).
35. Tak, P. P. et al. T cell subsets in osteoarthritis: from pathogenesis to therapeutic targets. *Nat. Rev. Rheumatol.* **16** (11), 667–680 (2020).
36. Otero, M. et al. Macrophage polarization in osteoarthritis: role of ROS and therapeutic implications. *Front. Immunol.* **12**, 737262 (2021).
37. Ji, Z. et al. Injectable hydrogel encapsulating siMMP13 with anti-ROS and anti-apoptotic functions for osteoarthritis treatment. *J. Nanobiotechnol.* **22** (1), 466 (2024).
38. Del Carlo, M., Schwartz, D., Erickson, E. A. & Loeser, R. F. Endogenous production of reactive oxygen species is required for stimulation of human articular chondrocyte matrix metalloproteinase production by fibronectin fragments. *Free Radic Biol. Med.* **42** (9), 1350–1358 (2007).
39. Salvemini, D. et al. Nitric oxide activates cyclooxygenase enzymes. *Proc. Natl. Acad. Sci. U S A*. **90** (15), 7240–7244 (1993).
40. Landino, L. M., Crews, B. C., Timmons, M. D., Morrow, J. D. & Marnett, L. J. Peroxynitrite, the coupling product of nitric oxide and superoxide, activates prostaglandin biosynthesis. *Proc. Natl. Acad. Sci. U S A*. **93** (26), 15069–15074 (1996).
41. Dai, S. M. et al. Catabolic stress induces features of chondrocyte senescence through overexpression of Caveolin 1: possible involvement of Caveolin 1-induced down-regulation of articular chondrocytes in the pathogenesis of osteoarthritis. *Arthritis Rheum.* **54** (3), 818–831 (2006).

Author contributions

CZQ wrote the main manuscript textZYZ, HCW, NL, RXL prepared Figs. 1, 2, 3, 4, 5, 6, 7, 8 and 9ZHW, BJW conducted data analysisNZ ensure the scientificity and reliability of the research, review and revise the content of the manuscript textAll authors reviewed the manuscript.

Funding

This study was not supported by any funding.

Declarations

Competing interests

The authors declare no competing interests.

Ethical approval and consent to participate

Ethical approval was obtained from the Ethics Committee of Affiliated Xinhua Hospital of Dalian University. Written informed consent was obtained from all participants.

Additional information

Supplementary Information The online version contains supplementary material available at https://doi.org/10.1038/s41598-025-11667-7.

Correspondence and requests for materials should be addressed to N.Z.

Reprints and permissions information is available at www.nature.com/reprints.

Publisher's note Springer Nature remains neutral with regard to jurisdictional claims in published maps and institutional affiliations.